

## Swimming behavior of larval *Pisaster ochraceus*

Silke Bachhuber<sup>1,2</sup> Jenna Sullivan<sup>1,3</sup>  
Professors: Danny Grunbaum and Richard Emlet

Larval Biology  
Summer 2014

<sup>1</sup>Friday Harbor Laboratories, University of Washington, Friday Harbor, WA 98250

<sup>2</sup>Department of Ecology, Evolution, and Marine Biology, University of California, Santa Barbara, Santa Barbara, CA 93117

<sup>3</sup>Department of Integrative Biology, Oregon State University, Corvallis, OR 97330

Contact:

S. Bachhuber: [bachhuber@umail.ucsb.edu](mailto:bachhuber@umail.ucsb.edu)

J. Sullivan: [jenna.sullivan@science.oregonstate.edu](mailto:jenna.sullivan@science.oregonstate.edu)

*Keywords:* *Pisaster ochraceus*, larval swimming, behavior, brachiolaria, modeling

## **Abstract**

The behavior of sea star brachiolaria larvae is poorly understood and the role of their elongated posterior processes in swimming is unknown. We attempt to characterize swimming speed and behavior in the late stage brachiolaria of *Pisaster ochraceus* in order to form a metric for larval health and to better understand the role of larval behavior in feeding and dispersal potential. We found that larvae swim faster in the presence of food and sink at a consistent rate when cilia are removed, which does not vary linearly with body or process length. In a simulation of simplified model brachiolaria in horizontal shear flow, larvae with their posterior processes parallel were more stable, while larvae with angled processes began to tumble at lower levels of shear. Further investigation will use video analysis to assess larval movement in varying levels of vertical shear that we created in a column using a rotating belt.

## **Introduction**

The dispersal and recruitment of free-spawning benthic invertebrate larvae to near-shore habitats is crucial to the population dynamics of intertidal and subtidal communities. However, factors that influence larval development and behavior are complex and relatively poorly resolved for many taxa. Biogeophysical models have traditionally considered planktonic larvae to move with ocean currents as passive particles, reflecting their characterization as ocean drifters or “wanderers.” Small-scale processes matter in larval distribution and recruitment dynamics (McManus and Woodson 2011, Pineda et al. 2009). For example, dispersal and settlement patterns can change significantly with the inclusion of larval behavior (e.g. Rothlisberg 1983, North et al. 2008), planktonic duration (e.g. Siegel et al. 2003) and body form (e.g. Deksheniaks et al. 1997) in geophysical models.

As larval bodies are typically denser than seawater, larvae must control their position in the water column to facilitate feeding and predator avoidance and to optimize advective transport (Chan 2012). The pelagic environment is often vertically stratified in resource availability, temperature, salinity, and advective flow. Consequently, vertical position in the water column has strong impacts on larval dispersal, growth and survival (Fisken et al. 2007, Chan 2012). Larval swimming behavior and response to water flow can be modulated by larval morphology and allow larvae to selectively regulate their positions in the water column (Grunbaum and Strathmann 2003, Clay and Grunbaum 2011). Larval movement independent of flow may be important for dispersal in currents and feeding in “patches” with high algal density (Metaxas and Young 1998).

Larval behavior also changes dramatically during development. Upward swimming appears to be advantageous for larvae at early stages of development (Staver and Strathmann, 2002), but downward movement via swimming or transport in downwelling water may be important for larvae nearing settlement (Roughgarden et. al. 1991, Grunbaum and Strathmann 2003). Additional morphological changes, such as the development of heavy structures like rudiments, may modify weight distribution and swimming behavior of larvae as they develop.

This study provides a preliminary assessment of the importance of morphology and swimming behavior in late-stage larval *Pisaster ochraceus* under varying environmental conditions. We use laboratory-reared brachiolaria larvae and model simulations to address the following questions: (1) does larval swimming speed and trajectory differ in the presence of food? (2) what is the passive sinking speed and orientation of de-ciliated larvae? (3) is there a stability advantage to parallel versus angled orientation of long processes in shear flow? And (4) how do brachiolaria behave in vertical shear, and do they tend to move into upwelling or

downwelling water? The motivation of this study, beyond basic investigation of poorly understood but ecologically important larvae, was to establish baseline behavioral and physical data on larvae of a sea star species that has been affected by the 2013-2014 outbreak of Sea Star Wasting Syndrome (SSWS). SSWS has decimated many sea star populations in the Northeast Pacific, and their recovery likely will depend in large part on the success of larval recruitment (Stokstad, 2014). However, impacts of SSWS on larvae are unknown. Behavioral data from this study will provide a sensitive assay, beyond simple measures of survival, of the effects of SSWS on larvae and can help predict potential for population recovery.

## **Methods**

### *Study organism*

Larvae of *Pisaster ochraceus* collected from Shady Cove, Friday Harbor, WA were spawned on June 19, 2014 and raised until the late brachiolaria stage (Fig. 1). Larval cultures were maintained in 0.45  $\mu\text{m}$  filtered seawater at ambient temperature (12-16 $^{\circ}$ C) and fed algal cultures of *Dunaliella tertiolecta* and *Rhodomonas lens* at a concentration of 7500 cells/mL every other day.

### *Behavioral assays*

We assessed larval swimming with food (control) and without food using two metrics: (1) average speed to swim 1.4 cm, and (2) trajectory at 10-second intervals over a two-minute observation period. For each metric, ten larvae were haphazardly selected, individually placed in a still water column (500 mL; Fig. 2) chilled to 12 $^{\circ}$ C, and allowed to acclimate for one minute before swimming performance was measured. Speed was measured as time taken to swim 1.4 cm (which never exceeded two minutes), and trajectory was characterized as upward, downward, sideways, or stationary. Food treatments consisted of *Dunaliella* algae at a density of  $\sim$ 7500

cells/mL, a density similar to that expected to be encountered by a larvae at the chlorophyll maximum during a spring bloom (Metaxas and Young 1998).

### *Sinking rate*

The role of ciliary motion in swimming was examined by removing cilia from larvae. Ten larvae were immersed briefly in double-strength filtered seawater (2x seawater: filtered seawater + 30 g/L NaCl) to remove cilia. Larvae without cilia were placed in the column without algae and their arm orientation and sinking speed over a distance of 1.4 cm was recorded three times per larva. Larvae were imaged under a dissecting microscope using an Infinity2 camera and InfinityCapture (version 5.1.0.3). Larval body length and arm length were measured in ImageJ (version 1.48)(see Fig. 1 for example body length measurement) after trials were completed to account for the effects of larval size on sinking speed. All of the larvae used in this trial survived treatment and regrew their cilia within 12 hours. We used a two-sample *t*-test to assess differences in mean swimming speed for larvae in the presence and absence of food.

### *Shear flows*

To assess larval swimming in shear flow, a column (4 cm x 3.4 cm x 24.7 cm) with a rotating belt fitted to the inside walls was built and placed in an isolating tank at 12° C (see Fig. 2). The belt was rotated at different speeds to generate three different shear treatments (low, medium, and high) at approximately 0.1 s<sup>-1</sup>, 0.14 s<sup>-1</sup> and 0.25 s<sup>-1</sup>, respectively. Approximately 0.5 mL *Rhodomonas lens* algae was added to visualize shear flows. For each behavioral trial, the belt was allowed to spin for one minute to allow flow to approach steady state before 15 larvae were added to the column and filmed for several minutes. Three groups of 15 larvae were filmed for each treatment with an Udoo microcomputer ([www.udoo.org](http://www.udoo.org)). We used Avidemux (v. 2) tracking software created by D. Grunbaum and Chris MacGregor (University of Washington,

2008) to analyze video and track motion of algal particles and larvae in column at different levels of shear. We then created maps of established shear gradients and larval trajectories using Tracker3D.

### *Hydrodynamic Model*

We created simplified models of *P. ochraceus* brachiolaria using FreeCAD software to compare larval stability with two common swimming morphologies and observed their stability in horizontal shear flow using a model developed in MATLAB by D. Grunbaum from the University of Washington (pers. comm.). Modeled larvae were uniformly ciliated and included a basic, slightly modified cylindrical body form with appendages constrained to approximate the two long arm processes held rigid at either parallel to the body or at 45-degree angles (Fig. 3). Based on measurements of 10 brachiopod larvae, arms measured approximately 81% of body length; the model reflected this ratio. Although brachiolaria arms are actively bent and moved during larval swimming, the model helps establish baseline levels of stability in shear and possible consequences of processes angle for swimming performance. Additionally, at low Reynolds numbers the transients in flow around arms are very brief. Hence, instantaneous swimming movements likely correspond closely to concurrent arm postures.

### **Results**

We observed one outlying observation of an abnormally fast larva in a trail without food. However, we believe that the recorded swimming speeds did not accurately reflect the mean speed of that larva as our timing periods happened to coincide with bursts of speed surrounded by periods of relatively slow swimming. Because *t*-tools are not resistant to outliers, we present the results both with and without this outlier, but interpret results without including this larva.

When we included the outlying observation of one unusually fast larval swimming speed under conditions without food, there was weak evidence for a difference in mean swimming speed with and without the presence of food (two-sample  $t$ -test  $p = 0.088$ ,  $df=18$ ). When that larva was excluded from analysis, swimming speed was significantly different in the presence of food (two-sample  $t$ -test  $p = 0.0005$ ,  $df=17$ , see Fig. 4). Mean upward swimming speeds were 0.24 and 0.39 mm/second for larvae in the presence of food and without food, respectively; larvae are estimated to swim between 0.07 and 0.22 mm/second faster in the presence of food (95% confidence interval). However, there were no significant differences in the proportion of time spent swimming up, horizontally, or remaining still between the feeding and non-feeding treatments (Wilcoxon rank sum test on horizontal swimming  $p = 0.93$ , remaining still  $p = 0.385$ ; proportion of observations observed swimming up were equal across treatments; Fig. 5). There was no effect of treatment on arm position (up or angled arms; Wilcoxon rank sum  $p = 0.125$ ). In both trials, larvae spent the majority of time (approximately 92% of observations) swimming up.

The sinking rate of de-ciliated larvae appeared to be independent of body length (see Fig. 6;  $R^2=0.0011$ ,  $n=10$ ). Sinking orientation was varied both across and within individual larvae: out of 30 observations of 10 larvae, 22 observations were made of larva orienting themselves to sink rudiment-first, five observations were made of sinking “headfirst” in the opposite orientation (in four separate larvae) and three observations were made of larvae sinking sideways (in three separate larvae).

Hydromechanical model results on larvae without a rudiment indicated that larvae are more stable with parallel long arm processes (Fig. 3B) than angled processes (Fig. 3A) and with processes trailing behind. Modeled larvae righted themselves to a “headfirst” sinking orientation (Fig. 3), and those with parallel processes had a threshold level of shear that initiated chaotic

tumbling that was 17% greater than that which initiated tumbling in the larva with angled processes ( $106 \text{ s}^{-1}$  and  $90 \text{ s}^{-1}$  respectively). The addition of a heavy rudiment would likely alter sinking orientation to the common, rudiment-first orientation observed in de-ciliated larval sinking trials. However, the degree of rudiment development may play a role in sinking orientation, which would impact performance in varying shear.

Maps of the shear flow created by our belt rotating at a low, medium, and high speed are presented in Fig. 7, 8, and 9, respectively. These figures are based on approximately ten seconds video clip selected from one run at each level of shear. We aimed to create consistent vertical shear that varied linearly in the horizontal direction. Although the gradient of shear increased more quickly with proximity to the belt (right side of Fig. 7C, 8C and 9C; the left side of the belt was outside of the field of view), based on velocity and trajectory of algal particles we succeeded in creating local maximum shear of at least  $0.5 \text{ s}^{-1}$ , which exceeded our projected maximum shear of  $0.25 \text{ s}^{-1}$  based on width and velocity of the belt. Future analysis will examine the paths taken by larvae in varying levels of shear, particularly incidence of movement across the column between upward and downward moving water, and the flow of water around individual larvae.

## **Discussion**

To our knowledge, this study represents the first attempt to quantify swimming behavior in *P. ochraceus* brachiolaria larvae in various environmental conditions. We provide preliminary information about the four questions posed in our introduction regarding brachiolaria swimming.

We found evidence that larval swimming behavior differs in the presence of food. The observed faster swimming in larvae with food may reflect the need to move water that has been cleared of food away from their bodies. More variable speed in the absence of food may reflect a “searching” behavior, such as area-restricted search, or other adaptations to maximize encounter

rate with algal prey or minimize encounters with potential predators. However, if food layers are stratified vertically in the water column, upward swimming would maximize encounter rate.

Further studies are needed to understand larval behavior within and outside of food patches.

Removing cilia from larvae and observing their sinking speed informs larval models and provides information about the roles of cilia and body structure in swimming. The lack of a linear relationship between body size and sinking rate may mean that body positioning while sinking plays a dominant role in sinking rate (as larvae were measured after sinking trials were completed). However, as larvae were photographed after completion of sinking trials, they may have changed their body position in the time (approximately 1-3 minutes) between trials and imaging. Further analysis of body position when sinking is needed to better determine the role of cilia in swimming.

Model results indicated a stability advantage in horizontal shear flow of long arm processes in parallel orientation rather than at 45-degree angles. Larvae with outstretched posterior processes tumble sooner in increasing shear flows, suggesting that parallel arm position and headfirst body orientation is more stable. Although brachiolaria processes are actively bent and moved during larval swimming, the model helps establish baseline levels of stability and likely consequences to swimming performance of angle of processes. Changing the position of the processes may confer increased stability and aid in swimming in various types of flows. More stable larvae may be able to feed, swim, and maintain position more effectively in shear flows such as those seen at upwelling and/or downwelling margins. However, our model results are restricted by the simplicity of the model used. In addition to simplified morphology and ciliary/arm movement, we did not take into account relative positions of the centers of weight and buoyancy, which likely influence larval stability particularly strongly in late-stage

brachiolaria with heavy developing rudiments. Differences in developmental stage or initial orientation may account for the variety of orientations observed in sinking, de-ciliated brachiolaria, but further study is necessary to accurately approximate force distribution on sinking, or swimming, larvae. Additionally, the establishment of larval trajectories in varying levels of shear, including tendencies to move into upward- or downward-moving water, will necessitate further video analysis of larval paths and their relation to water flow as measured by algal cell flow markers.

Understanding swimming behavior of these unusually-shaped larvae may inform both hypotheses about larval form and function as well as larval swimming behavior, feeding, and dispersion potential. Changing paradigms in larval biology emphasize the importance of behavior in different flows (i.e. upwelling vs. downwelling water) when estimating patterns of dispersal. In *P. ochraceus* and other northeast Pacific asteroid species, dispersal potential may be increasingly important given the impacts of a recent outbreak of Sea Star Wasting Syndrome, which has resulted in local extinction of many sea star populations along the US west coast intertidal and subtidal. Dispersal of larvae from populations with low incidence of wasting syndrome will likely be important for the recovery of *P. ochraceus* and other important sea star species in areas that have been decimated by the disease outbreak. Additionally, behavioral metrics provided in this study provide important baseline “normal” measurements with which to define potential effects of Sea Star Wasting Syndrome on larvae themselves.

## Works cited

- Clay, T., and D. Grünbaum. 2010. Morphology–flow interactions lead to stage-selective vertical transport of larval sand dollars in shear flow. *J Exp Biol.* **213**:1281-92.
- Deksheniaks, M. M., P.L. Donaghay, J. M. Sullivan, et. al. 2001. Temporal and spatial occurrence of thin phytoplankton layers in relation to physical processes. *Mar. Ecol. Prog. Ser.* **223**: 61–71.
- E. North, Z. Schlag, R. Hood et. al. 2008. Vertical swimming behavior influences the dispersal of simulated oyster larvae in a coupled particle-tracking and hydrodynamic model of Chesapeake Bay. *Mar Ecol Prog Ser.* **359**: 99-115.
- Fiksen, Ø, C. Jørgensen, T. Kristiansen et. al. 2007. Linking behavioural ecology and oceanography: larval behaviour determines growth, mortality and dispersal. *Mar Ecol Prog Ser.* **347**:195-205.
- Grünbaum, D, and R.R. Strathmann. 2003. Form, performance and trade-offs in swimming and stability of armed larvae. *J Mar Res.* **61**:659-91.
- McManus, M.A, and C.B. Woodson. 2012. Plankton distribution and ocean dispersal. *J Exp Biol* **215**:1008-16
- Metaxas, A, and C.M. Young. 1998. Responses of echinoid larvae to food patches of different algal densities. *Marine Biology* **130**: 442-445.
- Pineda, J., N.B. Reynolds, E. Victoria, et. al. (2012). Spatial connectivity and scaling: complexity and simplification in understanding recruitment in benthic populations. *Population Ecology* **51**:17–32.
- Rothlisberg, P. C. (1983). Modeling the advection of vertically migrating shrimp larvae. *J. Mar. Res.* **41**: 511–538.
- Roughgarden, J, T.M. Farrell, and D. Bracher. Cross-shelf transport causes recruitment to intertidal populations in central California. *Limnol. Oceanogr.* **36**: 279-288.
- Siegel, D. A., B. P. Kinlan, B. Gaylord, and S. D. Gaines. 2003. Lagrangian descriptions of marine larval dispersion. *Mar. Ecol. Prog. Ser.* **260**: 83–96.
- Staver, J. M. and R. R. Strathmann. 2002. Evolution of fast development of planktonic embryos to early swimming. *Biol. Bull.* **203**: 58 – 69.
- Stokstad, E. 2014. News Focus: Death of the Stars. *Science* **344**: 464-467.

## Figures

Figure 1: Brachiolaria larva with example length measurement shown in white and labeled rudiment and posterior processes.

Figure 2: Photo of experimental setup with chilled column and belt/motor generating shear flows and video apparatus in foreground.

Figure 3: Hydromechanical model of simplified *P. ochraceus* brachiolaria larvae including representation of general body form and long processes and more stable “headfirst” orientation in shear flows.

Figure 4. Average swimming speeds of larvae in the presence and absence of food particles (*Isochrysis galbana*) without outlying observation (n=10). The difference in mean swimming speeds is significant (two-sample t-test,  $p=0.0005$ ,  $df=17$ ).

Figure 5: Proportion of time spent swimming up, horizontally, or remaining stationary (“still”) for 10 different larvae at 10-second intervals over 2 minute observation periods in treatments with and without *Dunalella* algal cell food. Note the Y-axis: larvae spent most of their time swimming up. There were no significant differences in swimming trajectory across treatment (Wilcoxon rank sum test on horizontal swimming  $p = 0.93$ , remaining still  $p = 0.385$ ; proportion of observations observed swimming up were equal across treatments).

Figure 6: relationship between mean larval length (see Fig. 3) and sinking speed with cilia removed; there is no evidence for a linear relationship between mean length and mean sinking speed ( $R^2 = 0.0011$ ,  $n=10$ ).

Figure 7. Visualizations of water movement in the column at low level of shear, as tracked by algal cell trajectories during ten seconds of video. Part (A) shows paths taken by individual algal

particles. These paths were used to create the following maps: gradient of mean horizontal (B) and vertical (C) velocity of algal particles in the flow field; change in median horizontal component of shear in the (D) horizontal and (E) vertical directions; and changes in median vertical component of shear in the (F) horizontal and (G) vertical directions.

Figure 8. Visualizations of water movement in the column at medium level of shear, as tracked by algal cell trajectories during ten seconds of video. Part (A) shows paths taken by individual algal particles. These paths were used to create the following maps: gradient of mean horizontal (B) and vertical (C) velocity of algal particles in the flow field; change in median horizontal component of shear in the (D) horizontal and (E) vertical directions; and changes in median vertical component of shear in the (F) horizontal and (G) vertical directions.

Figure 9. Visualizations of water movement in the column at high level of shear, as tracked by algal cell trajectories during ten seconds of video. Part (A) shows paths taken by individual algal particles. These paths were used to create the following maps: gradient of mean horizontal (B) and vertical (C) velocity of algal particles in the flow field; change in median horizontal component of shear in the (D) horizontal and (E) vertical directions; and changes in median vertical component of shear in the (F) horizontal and (G) vertical directions.

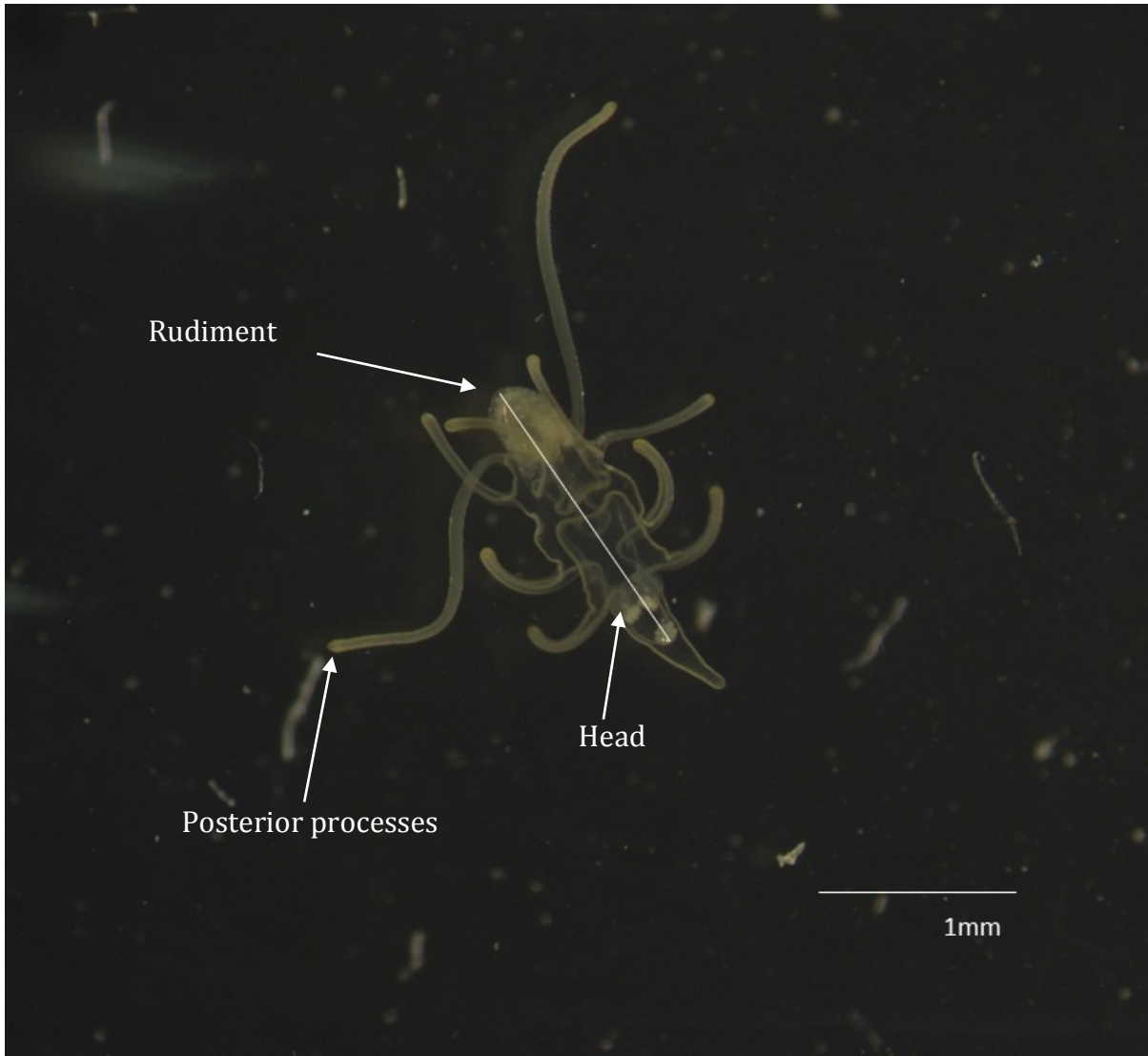


Figure 1

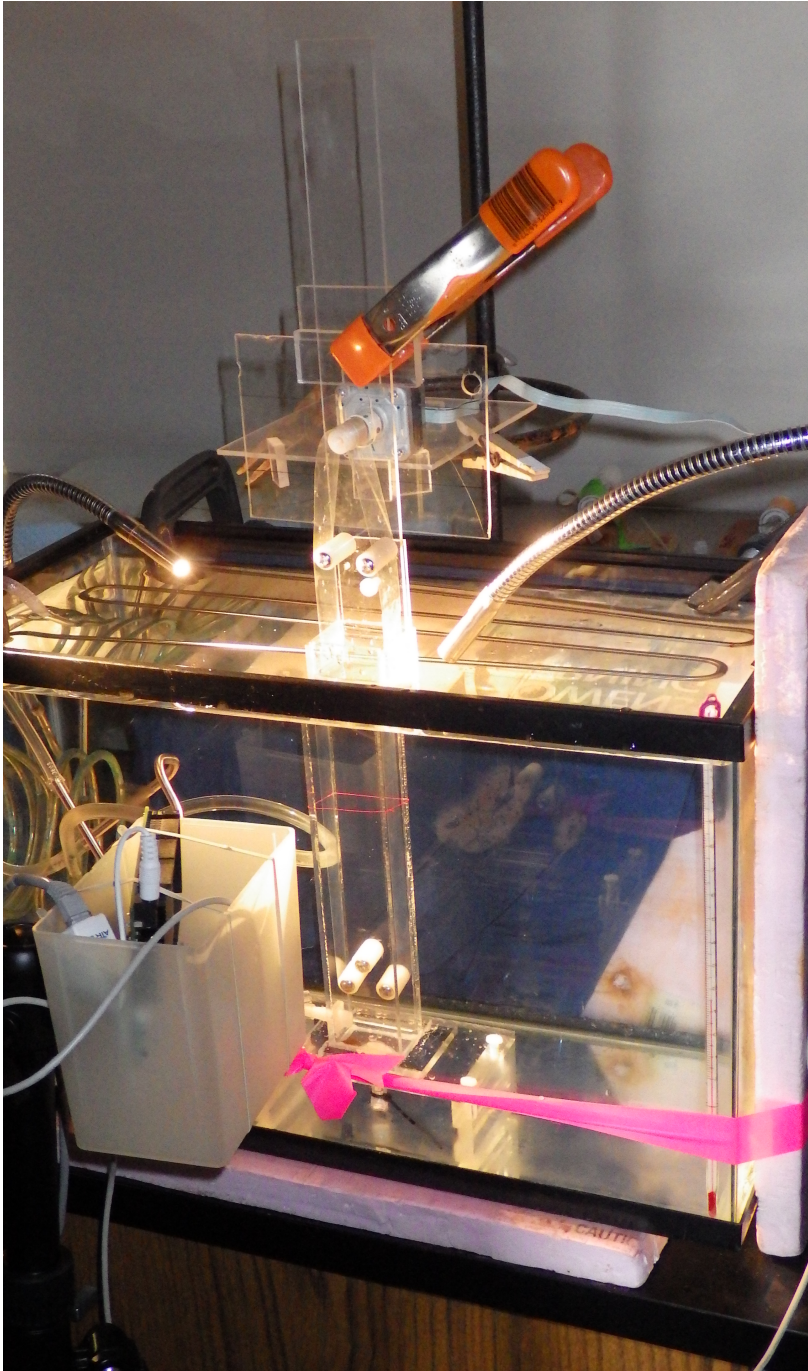


Figure 2

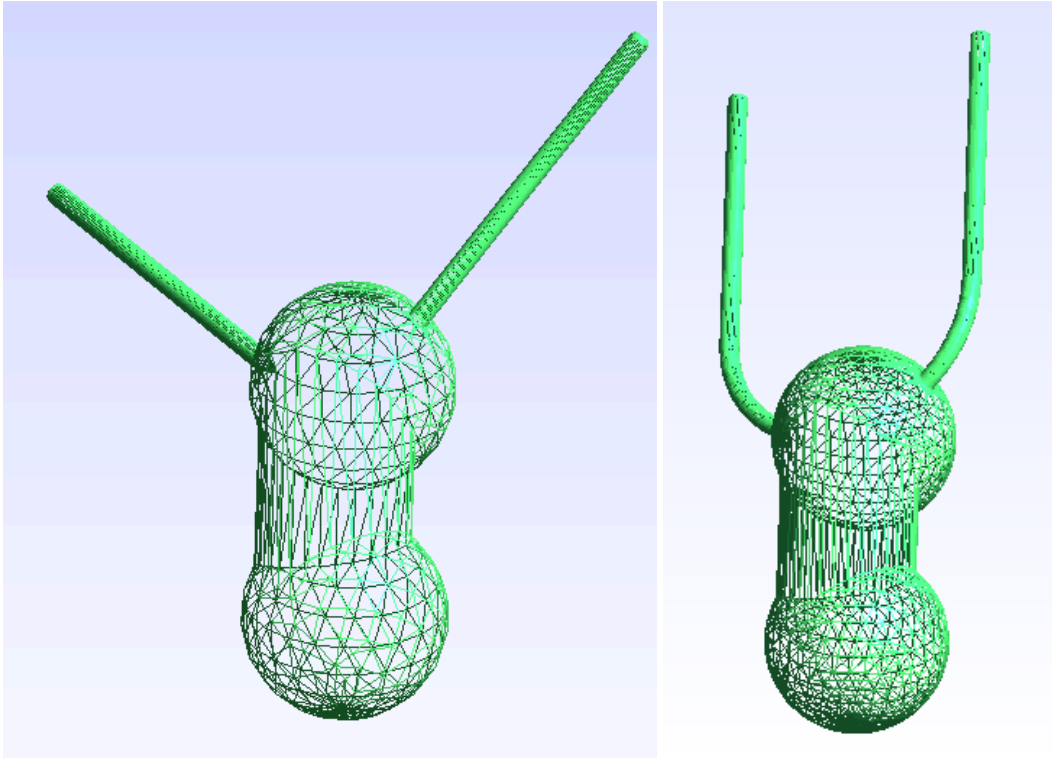


Figure 3

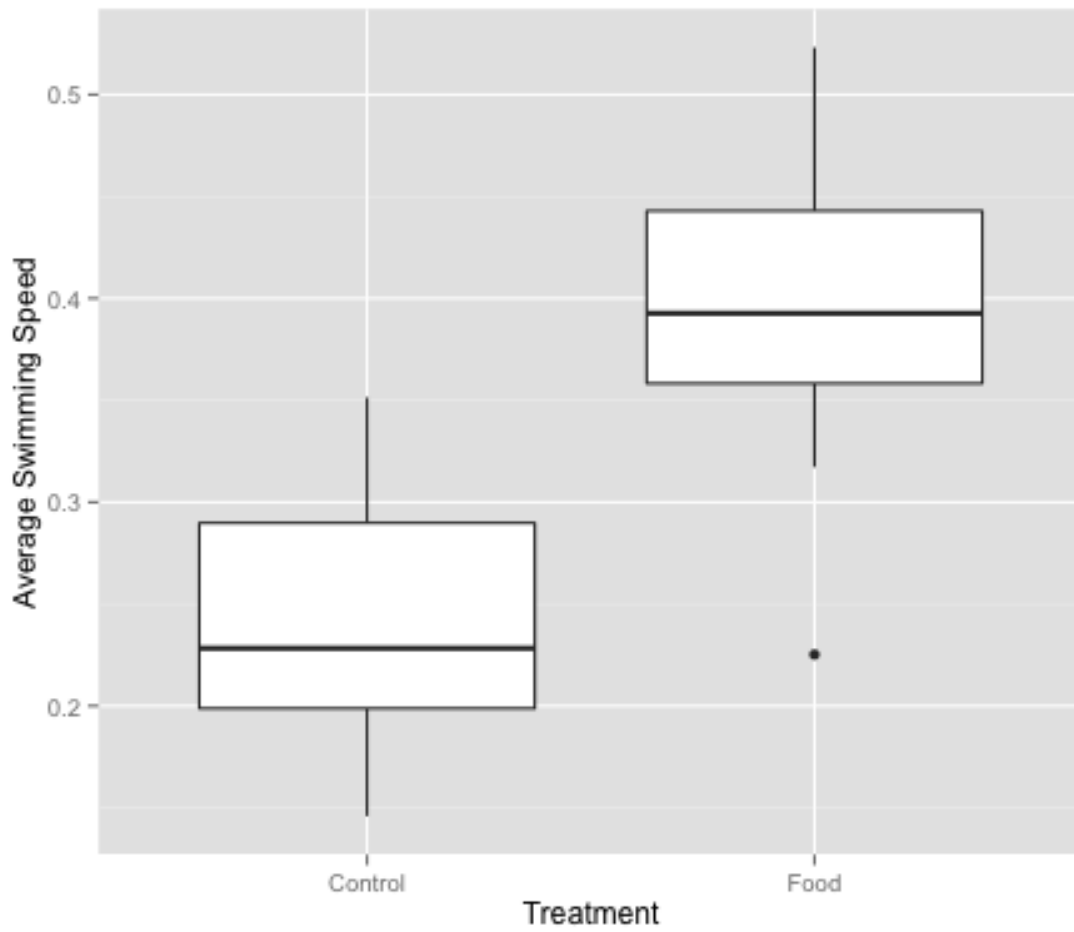


Figure 4

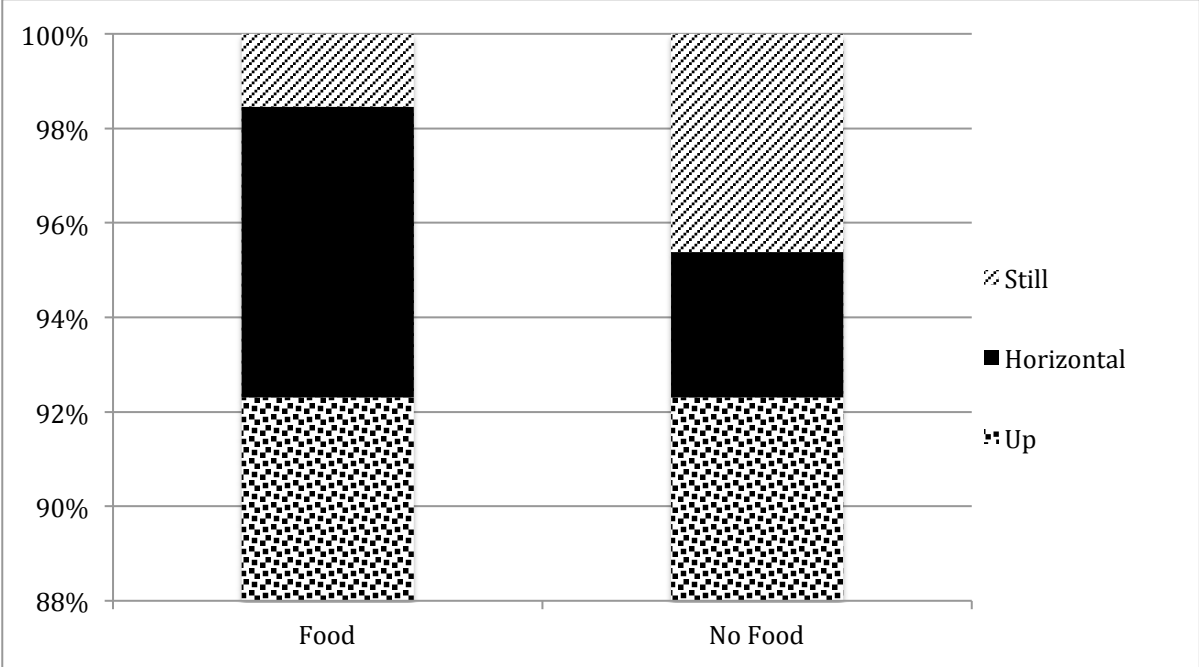


Figure 5

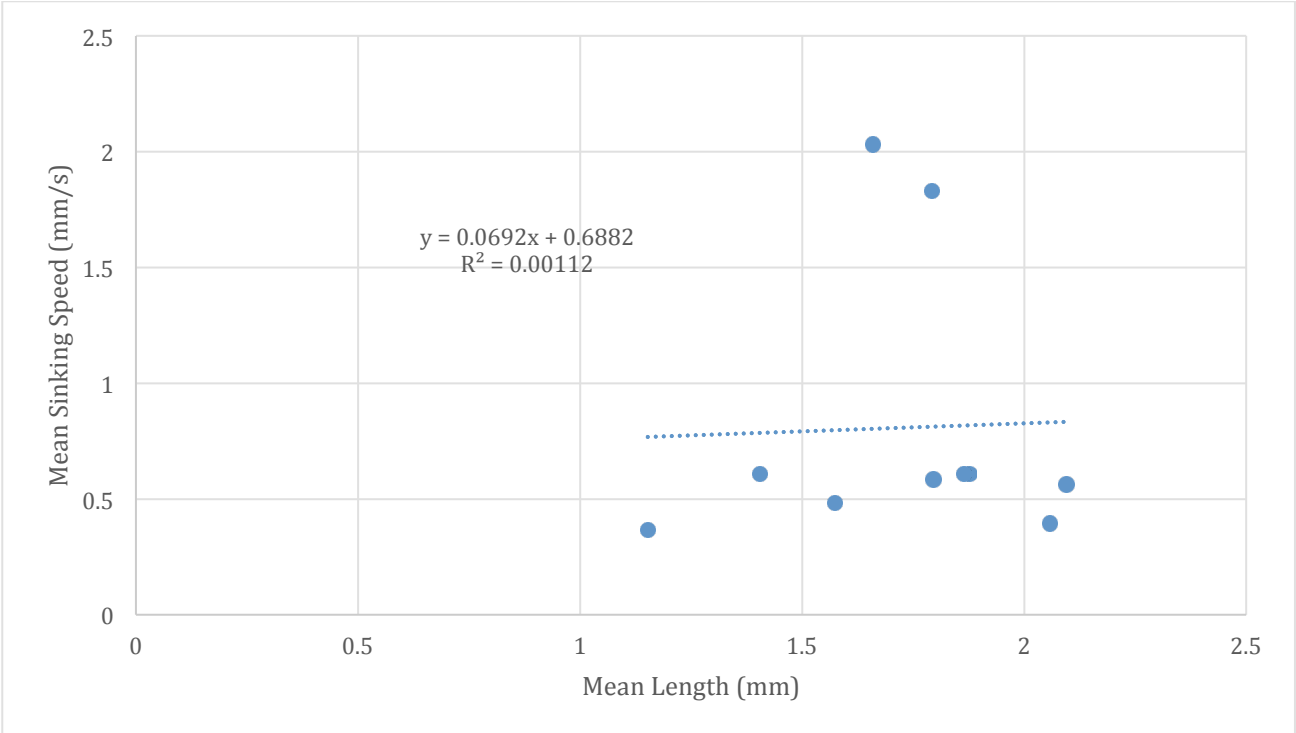
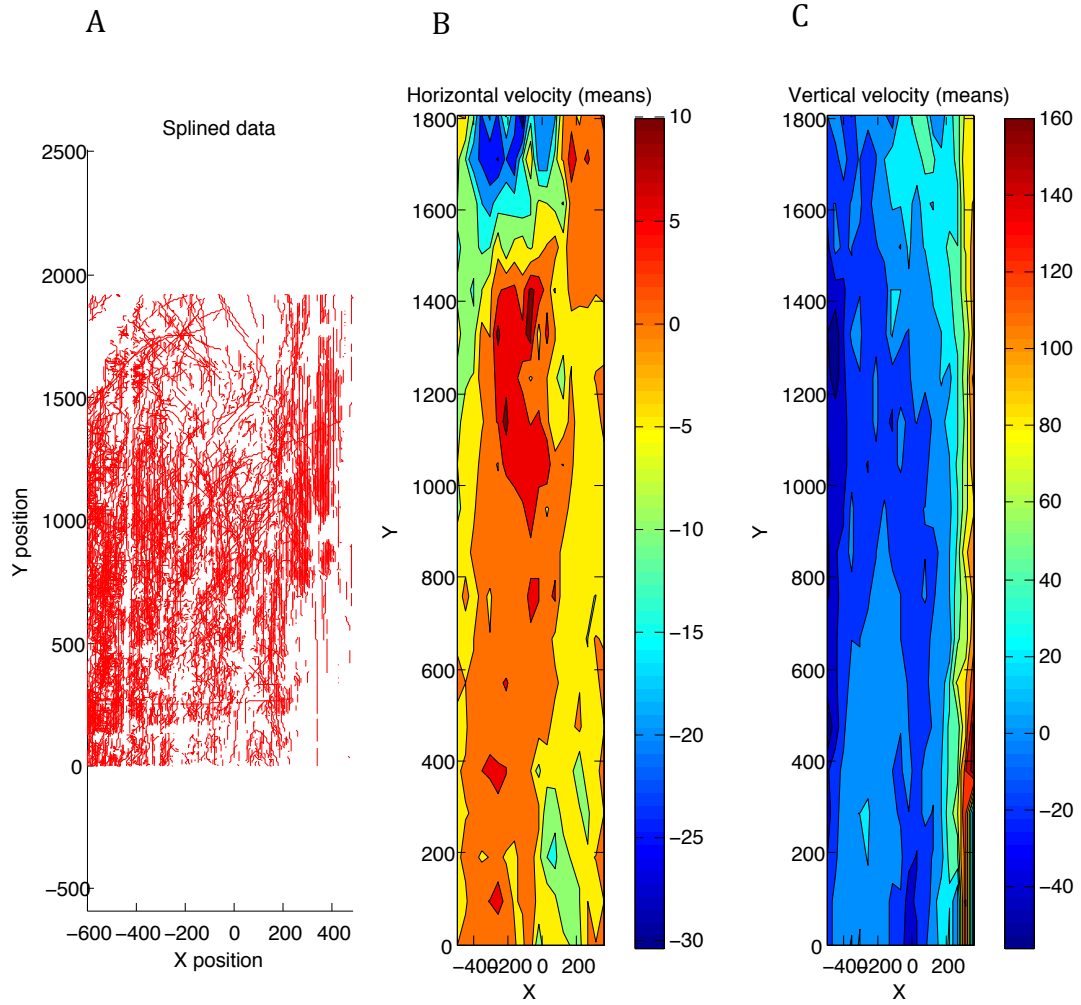
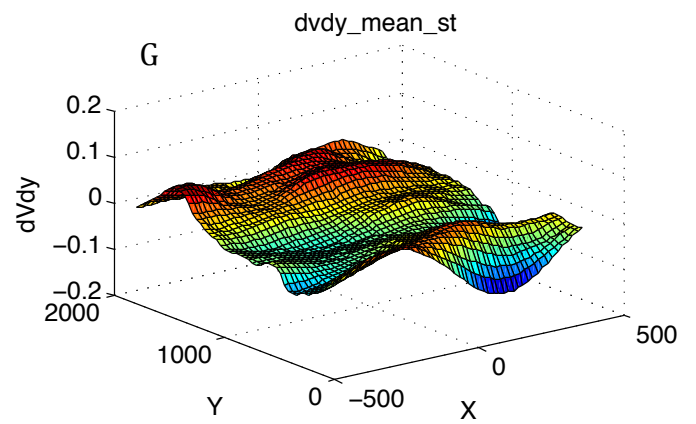
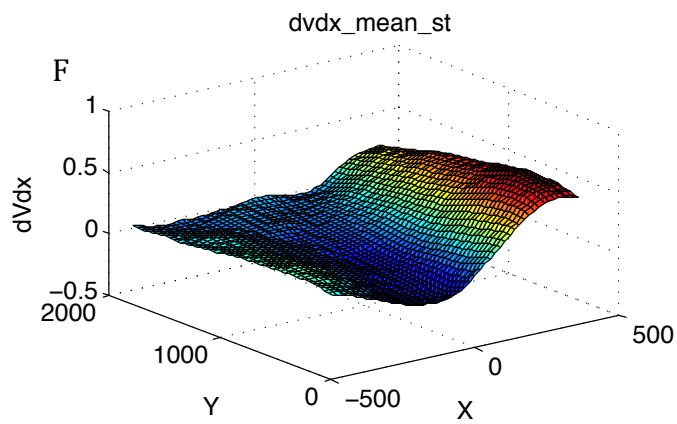
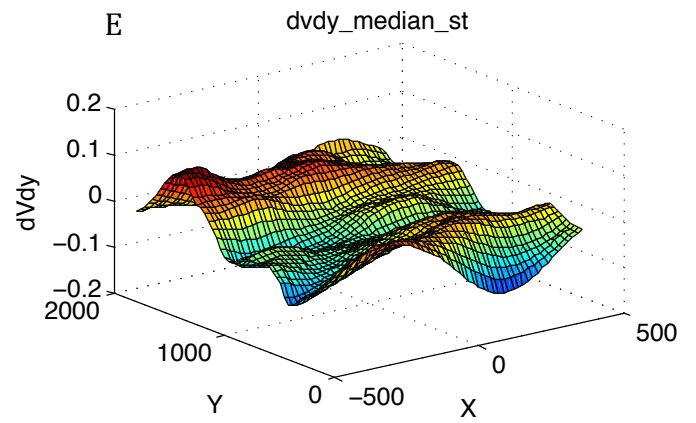
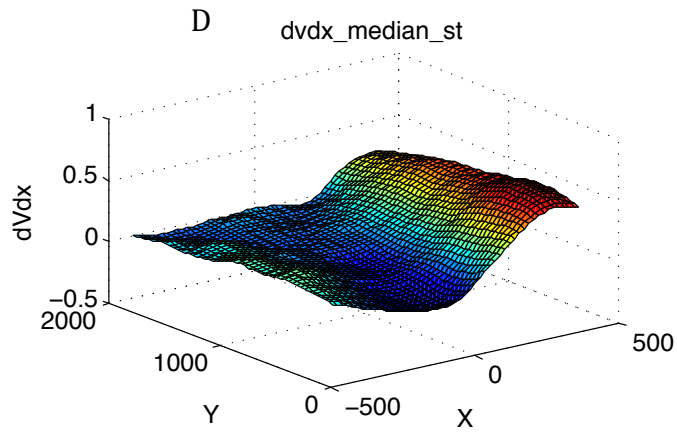


Figure 6





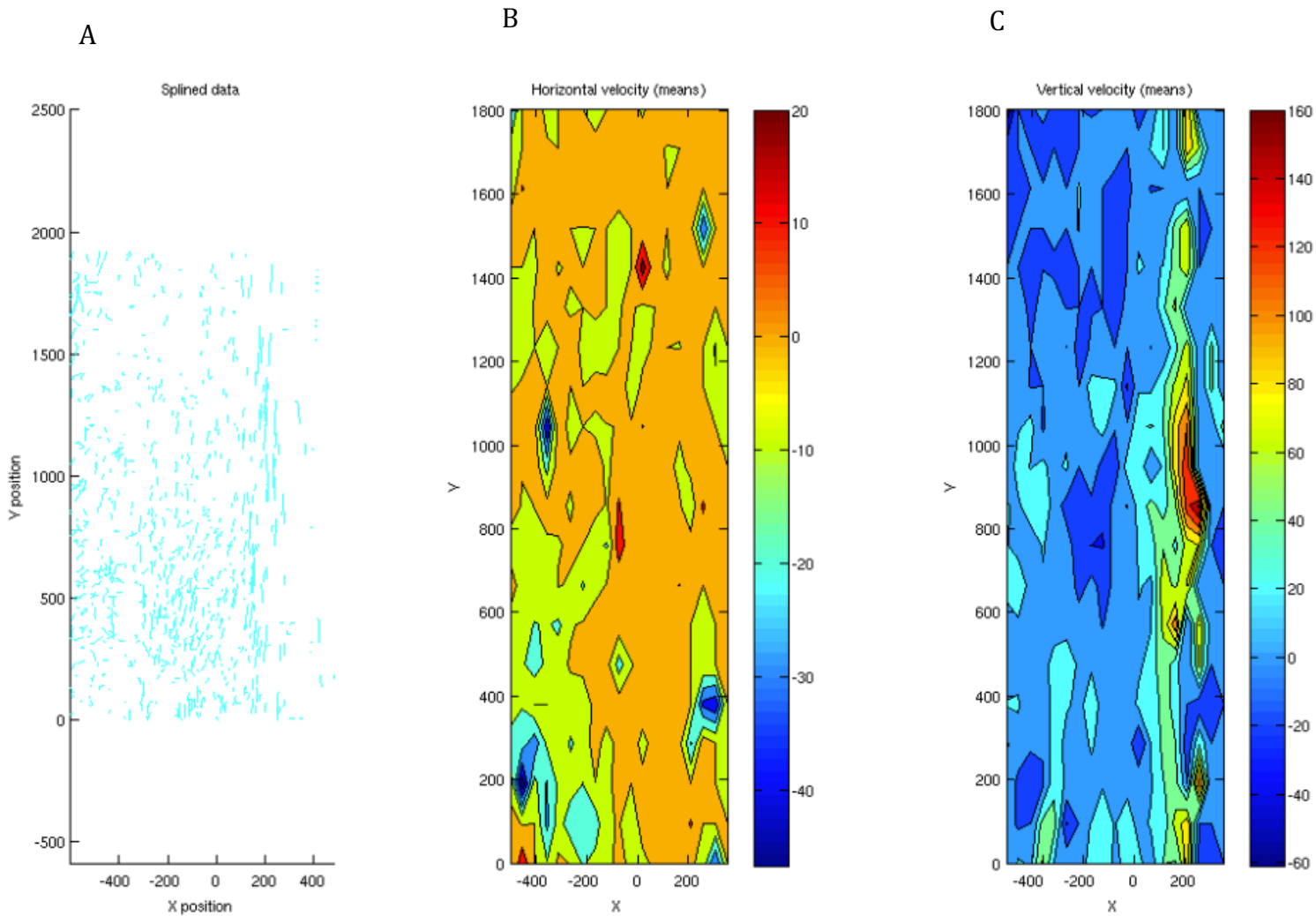


Figure 9 (parts A, B, C)

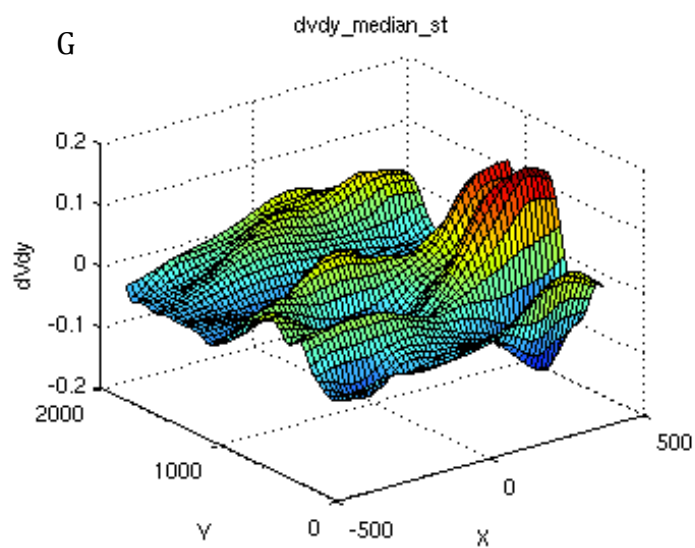
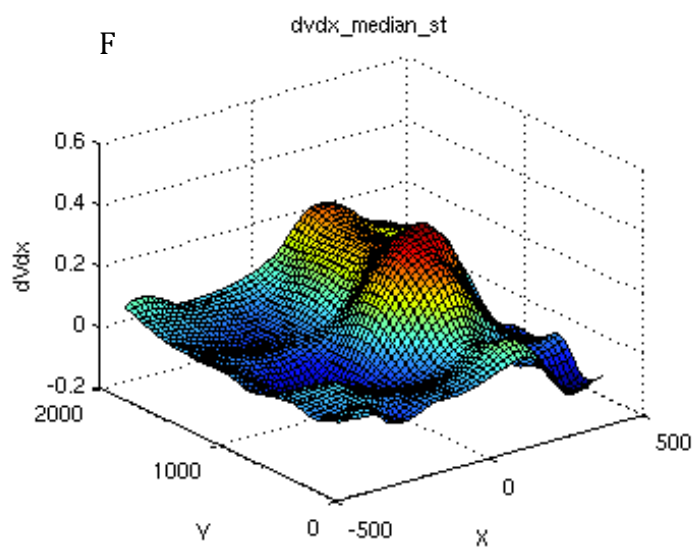
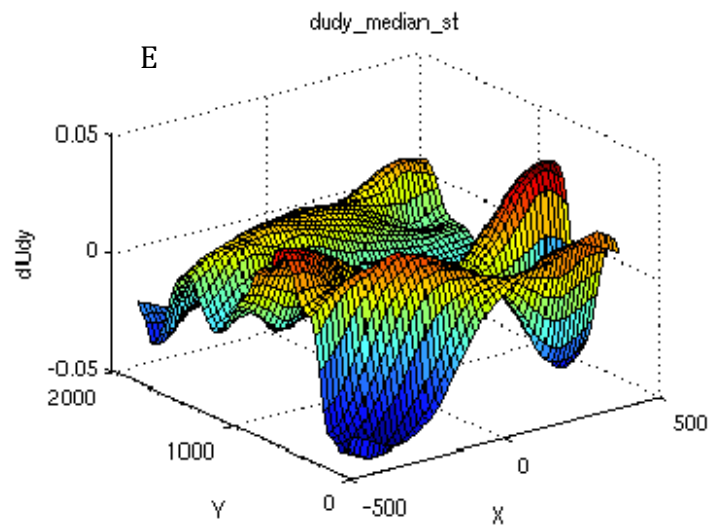
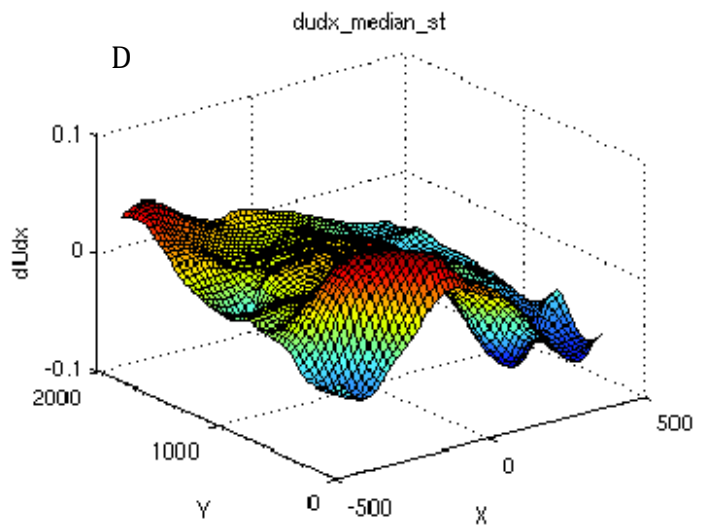


Figure 9 (parts D, E, F, G)

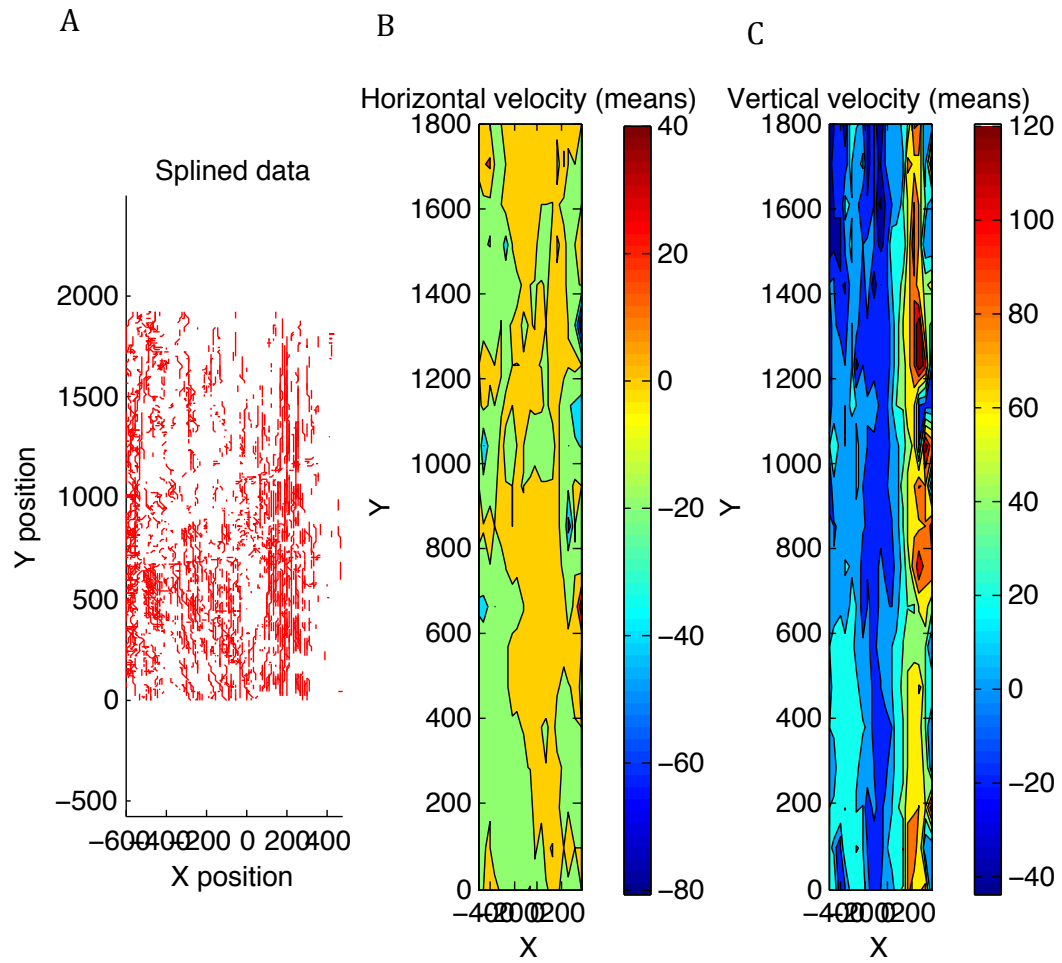


Figure 10 (parts A, B, C)

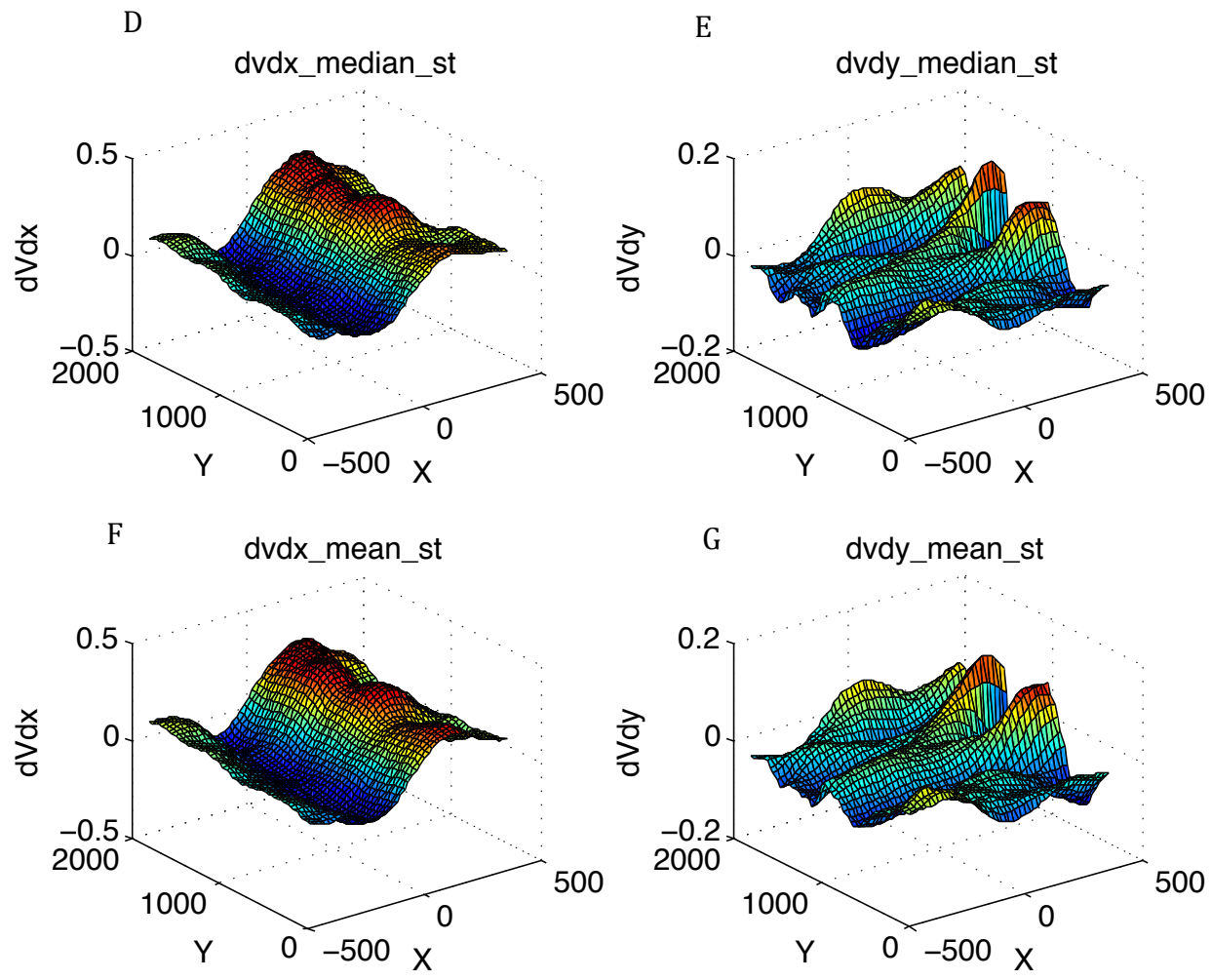


Figure 10 (parts D, E, F, G)